

# Instability Waves in the Tropical Pacific Observed with GEOSAT

Claire PERIGAUD

*Jet Propulsion laboratory, MS 300/323  
4800 Oak Grove Drive  
Pasadena, CA 91109, U.S.A.*

## ABSTRACT

Sea level variations for periods between 20 to 50 days are examined in the tropical Pacific ocean from Geosat data which have been processed and analyzed weekly during the first 13 months of the Exact Repeat Mission. Based on comparison with twice daily tide-gage data, sea level variations can be determined with an rms accuracy of 6 cm for time scales of a week. Subsampling by the satellite and smoothing introduced by the analysis aliase the frequency spectra by introducing artificial secondary peaks and reducing the energy level of significant peaks. However the synopticity of the satellite observations give significance to the energy peaks detected locally and allows a detailed description of the 20 to 50 days oceanic variations during 1 year. Along the equator, sea level spectra show low energy. The highest energy is found in the Northeastern Pacific along 5°N for 25 to 45 day periods, 1000 to 1500 km wavelengths, and a westward 40 km/day phase velocity. The signal filtered in this band of wavelengths and periods shows the strongest amplitude East of 160°W and the weakest amplitude along 2000 km in the Central Pacific. Waves are propagating energy eastward and are seasonally modulated in high correlation with the shear-strength of the zonal flows. West of the central zone of minimum amplitude however, the signal is no longer well correlated with the shear-strength variations. The signals at 5°N and 5°S are not antisymmetric with respect to the equator but positively correlated.

## I INTRODUCTION

Instability waves have been observed and simulated as wavelike oscillations in the meridional velocity along the equator and in the sea surface temperature about 2° north of the equator in the Northeastern tropical Pacific. Weisberg (1987) provides a synopsis of their theoretical and observational history. These oscillations are narrow-band in frequency and wavenumber with time and zonal length scales centered about 30 days and 1000 km respectively. Their phase speed is westward and their apparent group velocity is eastward. These characteristics fit the Rossby-gravity wave ones. The pressure field of such a theoretical wave is antisymmetric with respect to the equator. Maximum of wave amplitude in the dynamic topography has been observed in the Northeastern tropical Pacific with inverted echo sounders (Miller et al, 1985) and with Seasat altimeter data (Malarde et al, 1987). The packet duration of these oscillations is seasonally modulated and these waves seem to be generated by the (zonal or vertical) shear instabilities of the zonal equatorial currents (Cox, 1980). It seems clear that these instability waves play a primary role in the momentum balance of the near surface near equatorial mean currents. It is suggested that they may have similar importance for the near surface heat balance through meridional heat convergence towards the equator (Hansen and Paul, 1984).

The generation and decay of these energetic oscillations and the relation of their spatial and temporal distributions with the variations of the equatorial currents are addressed in this work. The Geosat altimeter data from the first year of exact repeat mission are processed and analyzed in the 20° band across the Pacific. Results are validated by



F 30 250

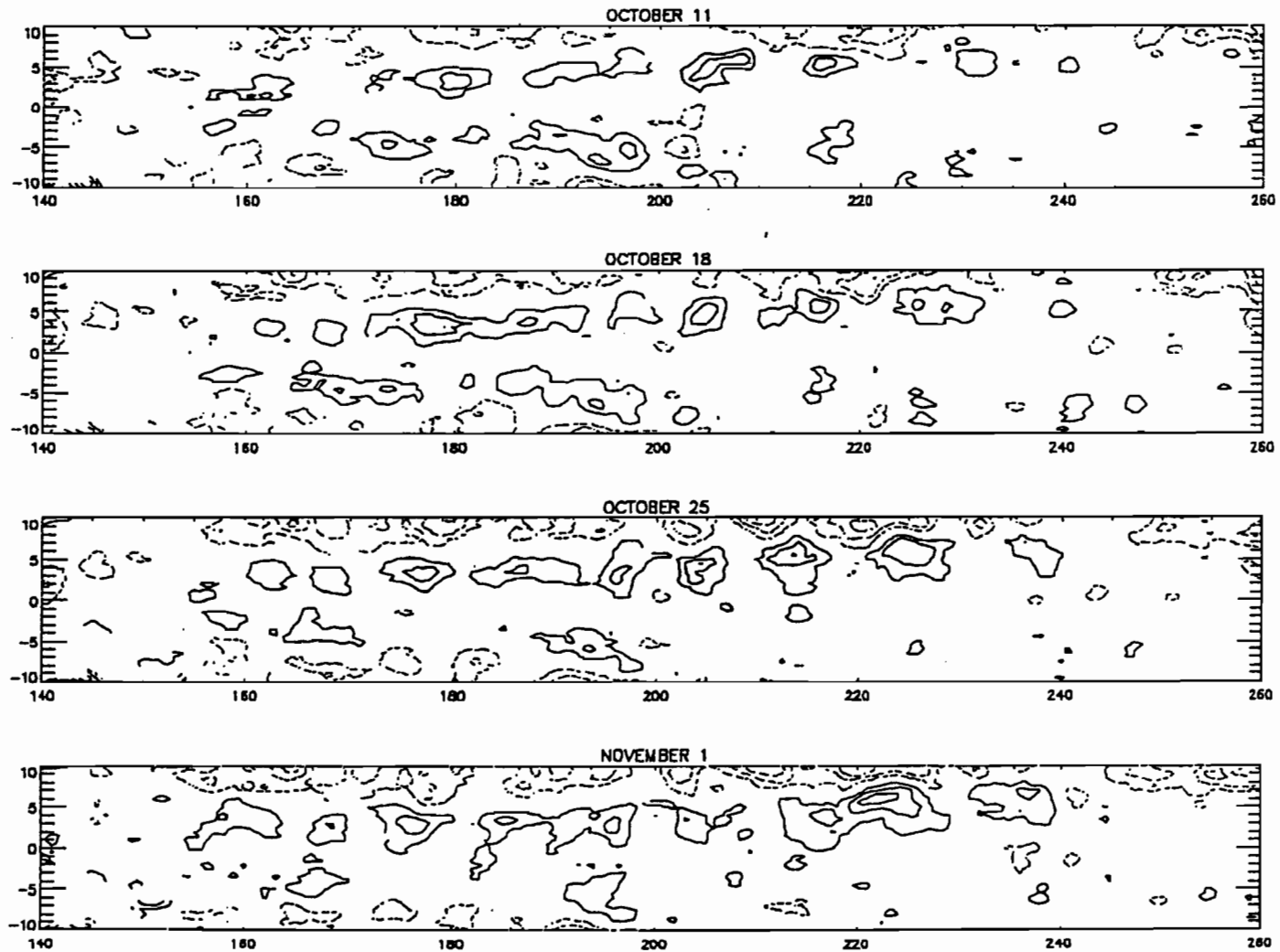


FIG.1. Weekly maps of sea level anomalies (relative to the 13 month mean) analyzed from GEOSAT altimeter data. Isocontours are 5 cm with continuous lines for positive and dotted lines for negative values. Zero contour is not drawn for more clarity.

comparison with tide-gage data. Frequency-wavenumber spectra are given as a function of latitude and altimeter signal filtered at the wave energy peaks is examined.

## II ALTIMETER DATA PROCESSING AND ANALYZING

The Geophysical Data Record computed by NOAA's National Geodetic Survey (Cheney et al, 1988) are corrected for earth and ocean tide, inverse barometer response of sea level to atmospheric pressure, wet (FNOC) and dry tropospheric path delays. Spikes are eliminated and data are gridded as a function of latitude along repetitive tracks of one ground "pass". Orbit errors are then corrected by applying to each repeat of each pass, a second degree polynomial between 20°S and 20°N, using the mean of the differences to the most complete pass (as used in Zlotnicki et al, 1989). The mean is taken from November 8 1986 to December 20 1987 (first 24 cycles).

Residual orbit error is negligible over a narrow latitudinal band as studied here. Presence of wet tropospheric signal is surely effective in the tropical band (Emery et al, 1988). However, little contribution of this signal is expected in the range of wavelengths, periods and propagation speeds typical of the oceanic variations that are investigated in the present study.

Residual alongtrack altimetric differences are then analyzed using a successive correction method, as formerly used in meteorology (Tripoli and Krishnamurti, 1975). The spatial resolution chosen is  $d = 0.5$  degree in latitude and longitude. This fine resolution results from a choice between the satellite crosstrack sampling (between 0 and 170 km at worst) and alongtrack sampling (7 km). The correlation function used in space is the Cressman function:

$(r^2 - R^2)/(r^2 + R^2)$  where  $r$  is the distance between the data point and the analyzed point and  $R$  is the correlation distance. Different sets of values for  $R$  have been chosen ranging from (4d, 3d, 2d, d) to (8d, 6d, 4d, 2d). An influence time of 34 days and an e-folding time of 5 to 7 days are applied on the weekly analyses performed over the 13 months of data. The time resolution (7 days) is chosen better than the satellite repetitive period (17 days) because oceanic information can be gained from neighbouring tracks within the satellite subcycle (3 days). This analysis is not optimal. It does not impose a westward phase speed as done with optimal analysis in (Malarde et al, 1987), nor any dynamical constraint as done with Kalman filter in (Gaspar and Wunsch, 1989). The present method certainly can be improved when the knowledge about the kinematics and physics of these waves becomes better.

A series of the sea level anomaly maps resulting from the Geosat analysis is presented in autumn 1987 (figure 1) showing succession of positive anomalies in the 3°N to 8°N latitudinal band. Some of them can be followed to migrate westward from week to week. Indeed the axis along which the anomalies are aligned, is not purely zonal but has a prevailing southwest-northeast orientation as has the axis of maximum shear-strength between the North Equatorial Counter Current and the South Equatorial Current (Kendall, 1970). However it is difficult from these results to characterize the waves involved in those variations as the anomaly maps represent the sum of the short-term, seasonal and interannual variations for this particular year. Taking monthly averages and spatial smoothing over 1° latitude and 4° longitude of these series allow us to recover the sea level variations that have been described for the year 1986-1987 (Cheney and Miller, 1987). The present series enhances the important contribution of the short-term events in the seasonal variations of the tropical Pacific Ocean. These short-term variations detected by the satellite are validated in the next section.

## III COMPARISON WITH TIDE-GAGE DATA

Tide gage data have been provided by Klaus Wyrтки on four island sites in the Central Tropical Pacific. These are twice daily data from November 1 1986 till December

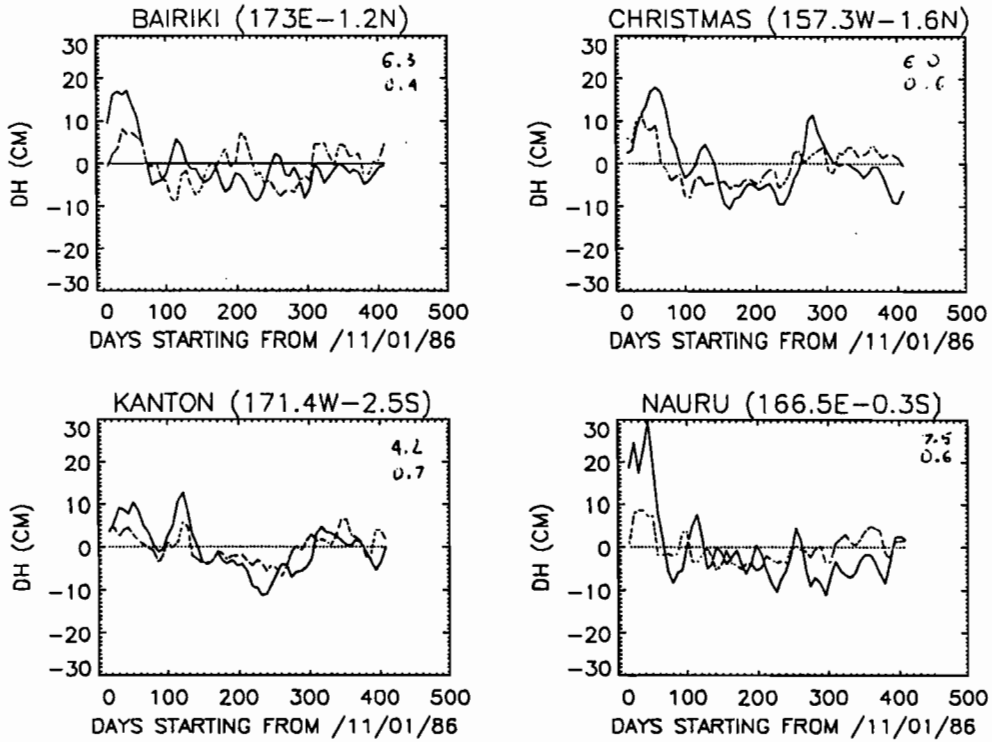


FIG.2. Variations of sea level relative to the 13 month mean derived from tide gage (continuous line) or from GEOSAT data (dotted line). The top value is the RMS difference between the 2 curves. The bottom value is the correlation coefficient.

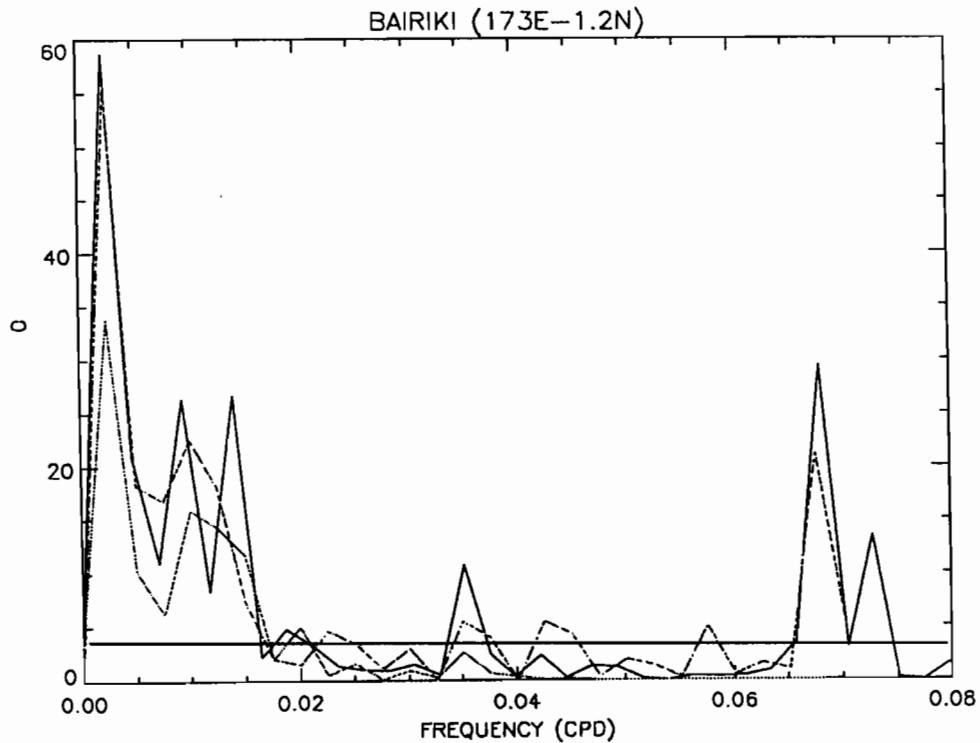


FIG.3. Frequency energy spectrum at Bairiki island derived from tide-gage data, with twice-daily data (continuous line), weekly subsampled data (dashed line) or 14 day averaged data (dotted line). The 95% level of confidence is given for the twice-daily data.

31 1987. The same 13 months mean is removed from these data and a 14 day running average is applied to remove the fortnight tidal signal. Then a weekly binning at the times corresponding to Geosat analyzed series is performed. The closest point within a 0.5 degree box around the island is extracted from the Geosat field for comparison. The time series (fig 2) agree within a mean RMS of 5.2 cm and a correlation coefficient ranging from 0.4 to 0.7. When the monthly mean is taken from both these series, the agreement is slightly better (mean RMS of 3.6 cm and correlation ranging from 0.1 to 0.8) and is a little less good than what Cheney et al (1989) found when comparing 16 sites of monthly averaged tide-gage data with Geosat over 18 months in 1985-1986 (respectively 3.7cm and 0.69). The energy spectrum of the non-smoothed non-subsampled tide-gage sea level presents 2 significant peaks at 14 days and 28 days. The former peak corresponds to a fortnightly tidal signal as found in Mitchum and Lukas (1987). The spectrum is modified by subsampling and smoothing (fig 3). Weekly subsampling twice-daily tide-gage data shifts energy from the higher frequencies into the lower ones so that artificial peaks show up in the 10 to 30 day range. Running a 14 day average on the twice-daily tide-gage data zeroes the fortnightly tidal signal but also reduces the 28 day signal just below the 95% level of confidence. These effects explain the differences between tide-gage and Geosat spectra (fig 4). Geosat peak has the energy level as the smoothed tide-gage peak, which has 50% less energy than the original one. Geosat spectra show secondary peaks between 10 and 30 days consistent with the subsampling aliasing. It is surely unfair to derive conclusions from these punctual comparisons all the more as these islands happen to be in the Central Pacific where the variance is the smallest (Wyrki, 1975). However Geosat series provide 300 grid points in longitude over which frequency spectra can be computed. Therefore the spatial consistency of the Geosat spectra can be examined.

#### IV WAVENUMBER-FREQUENCY SPECTRUM

Frequency spectra have been averaged in the Eastern (100°W to 160°W) and in the Western (140°E to 160°W) basins along zonal sections of the Geosat weekly series (fig 5). These basins have the same spectra along the equator, with a low of energy between 30 and 50 days, the highest energy level of all the spectra at the lowest frequencies and a secondary peak at 22 days just above the 95% level of confidence. The eastern basin presents significant peaks in the 25 to 45 day band both North and South of the equator. The peak maxima are centered on 33 days at 5°N and 40 days at 5°S and the secondary maxima centered at 7.5°N and 7.5°S with a wider frequency band shifted to the longer 40 day periods. The energy level is about twice larger in the North than in the South. The 25 to 45 day peak may be due to instability and will be studied in the next section.

The equator presents a minimum of energy in the 30 to 50 days as the Rossby-gravity wave has a zero sea level amplitude along the equator. The secondary peak at 22 day can be due to subsampling of the highest frequency waves which energy is concentrated in the equatorial wave guide.

In the western basin, significant peaks show up between 40 and 60 days but little energy is found below 35 days. The structure looks more complex than in the East and is certainly resulting from the superposition of different events. The increase in the periods from East to West has been observed in current measurements (Halpern et al, 1988) and tide-gage data (Chriswell and Lukas, 1989) and corresponds to the eastward dispersion of the Rossby-gravity wave. Two main differences appear between these spectra and those derived from 730 days of 17 tide-gage stations in the central and western 10°S to 10°N Pacific (Mitchum and Lukas, 1987). No 40 to 50 day peak is found along the equator and the 20 to 40 day peak is centered higher than 30 days rather than lower. The peak, which corresponds to sea level response to atmospheric oscillations (Enfield, 1987) may be absent on 1986-1987; indeed it has not either been observed in the Western Pacific Ocean for 1986-1987 (McPhaden et al, 1989).

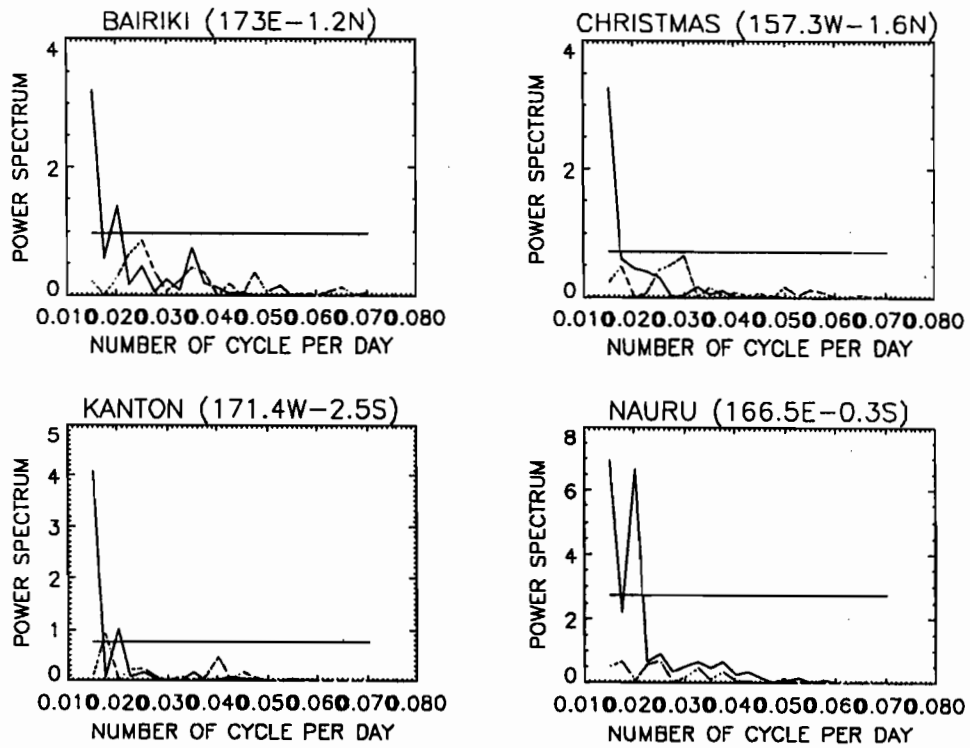


FIG.4. Frequency power spectra in  $\text{cm}^2/\text{cycle per day}$  derived from tide-gage smoothed data (continuous line) and from GEOSAT data (dotted line). The 95% level of confidence is given for the twice-daily tide-gage data.

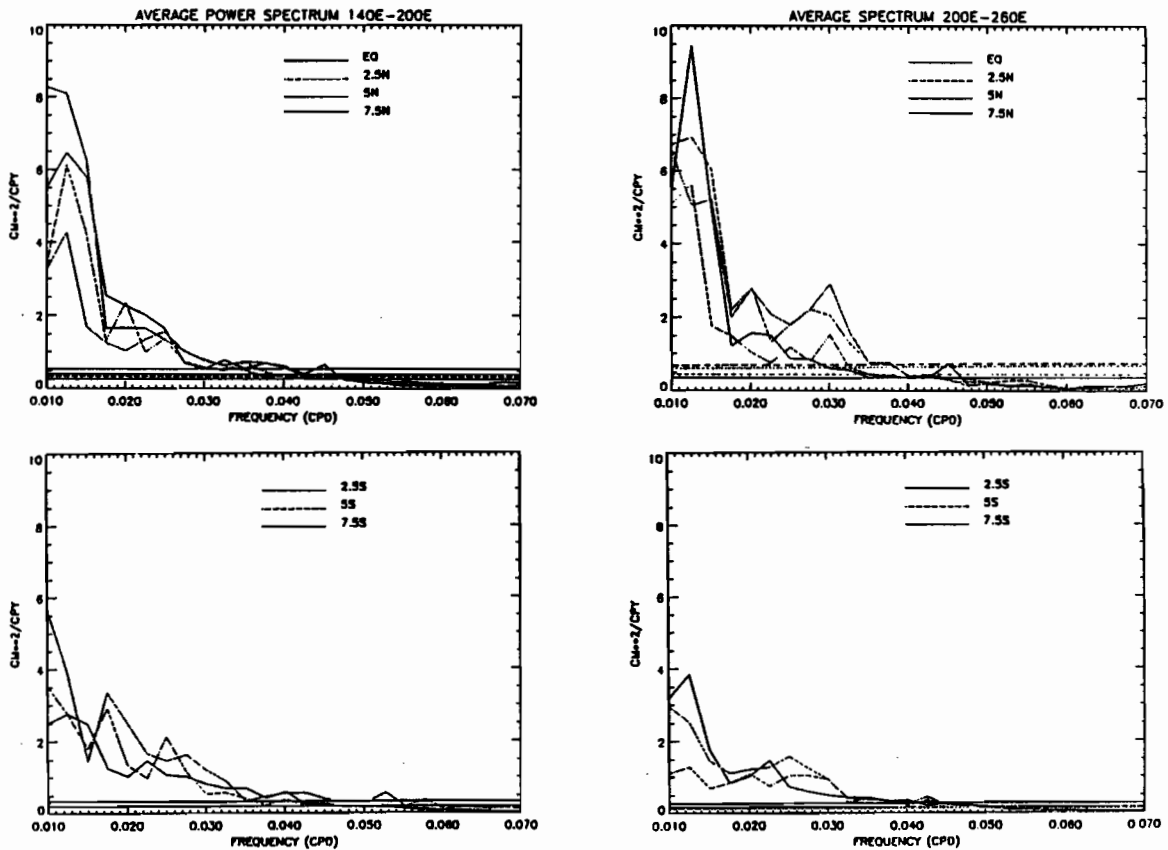


FIG.5. GEOSAT frequency power spectra averaged along zonal sections in the western and eastern Pacific. Units are cycle per day for frequencies and  $\text{cm}^2$  per (cycle per year) for power.

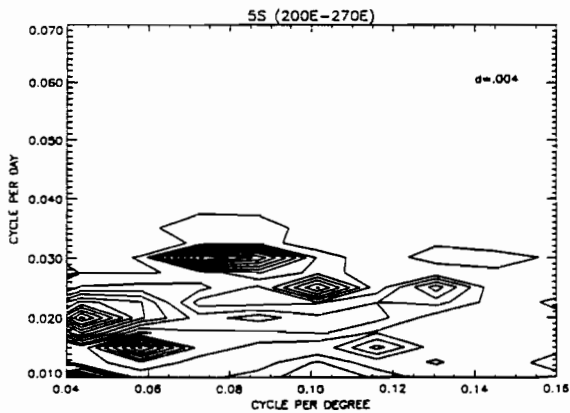
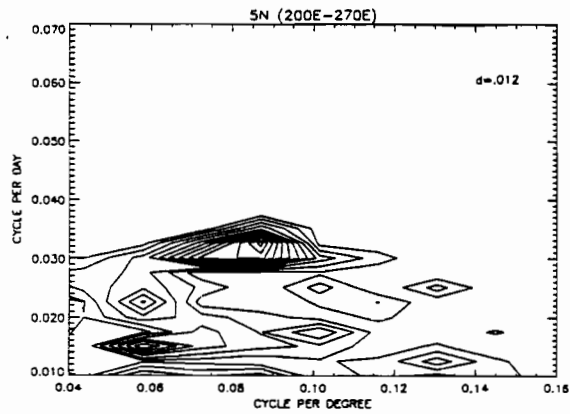


FIG.6. Wavenumber-frequency spectra derived at 5°N and 5°S zonal sections of GEOSAT anomaly maps. Units of isocontours are in  $\text{cm}^2$  per (cycle per year) per (cycle per km).

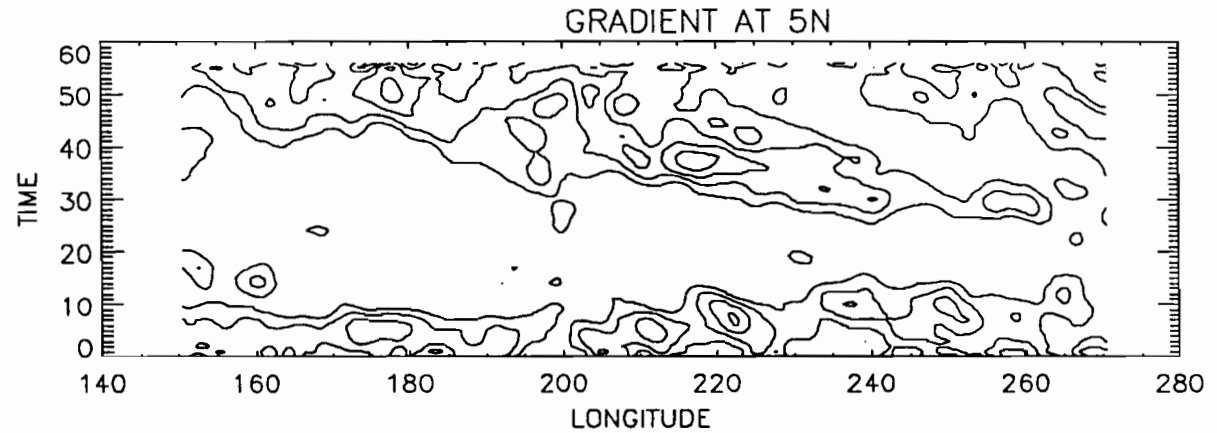
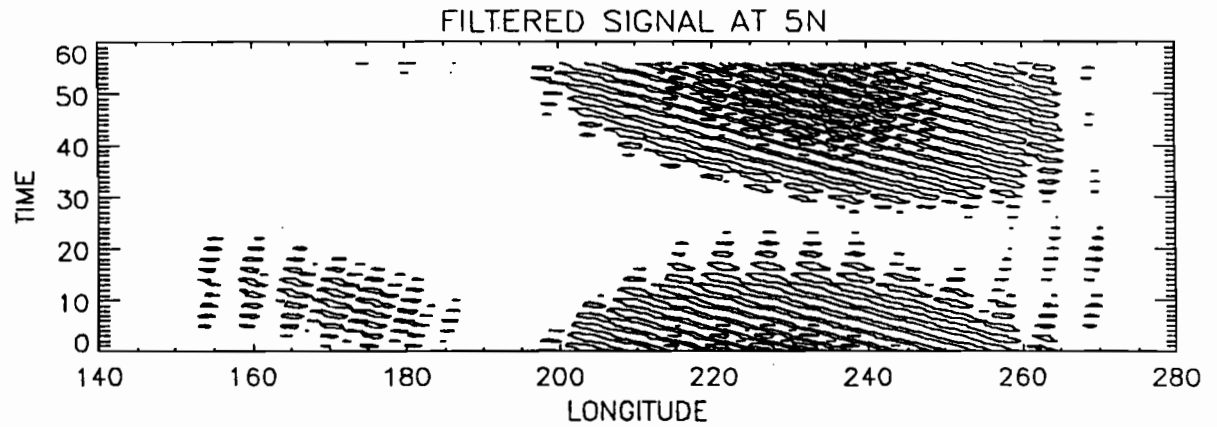


FIG.7. Top: Amplitude of GEOSAT filtered sea level variations at 5°N as a function of longitude and time (units of time axis are week starting on November 16 1986 and isocontours are 0.5 cm).  
Bottom: meridional sea level gradient (relative to the 13 month mean): only the negative values increasing the shear-strength are contoured. Isocontour is 2 cm per degree of latitude.

Wavenumber frequency spectra are then given at 5°N and 5°S (fig 6). The 25 to 45 day band corresponds to the 1000-1500 km zonal wavelength range. Some symmetry relative to the equator is found as well in these wavelength band, but with less energy in the Southern than in the North.

## V FILTERED SIGNALS

Geosat analyzed residuals are filtered within 25 to 45 days and 1000 to 1500 km. The filtered signal (fig 7 top) clearly shows a westward phase speed of 40 km/day. From November 1986 to February 1987, waves are present in the western and eastern Pacific with the strongest amplitude in the East and the weakest amplitude in the Central Pacific between 160°W and 180°. The maximum amplitude in time is 4 cm East of 180° and 2 cm in the West. The eastern and the western packets of waves are disconnected. Waves are the weakest between February and June and become active again in the East from 120°W in June to 160°W in August. Very little wave activity is found in the West after February 1987.

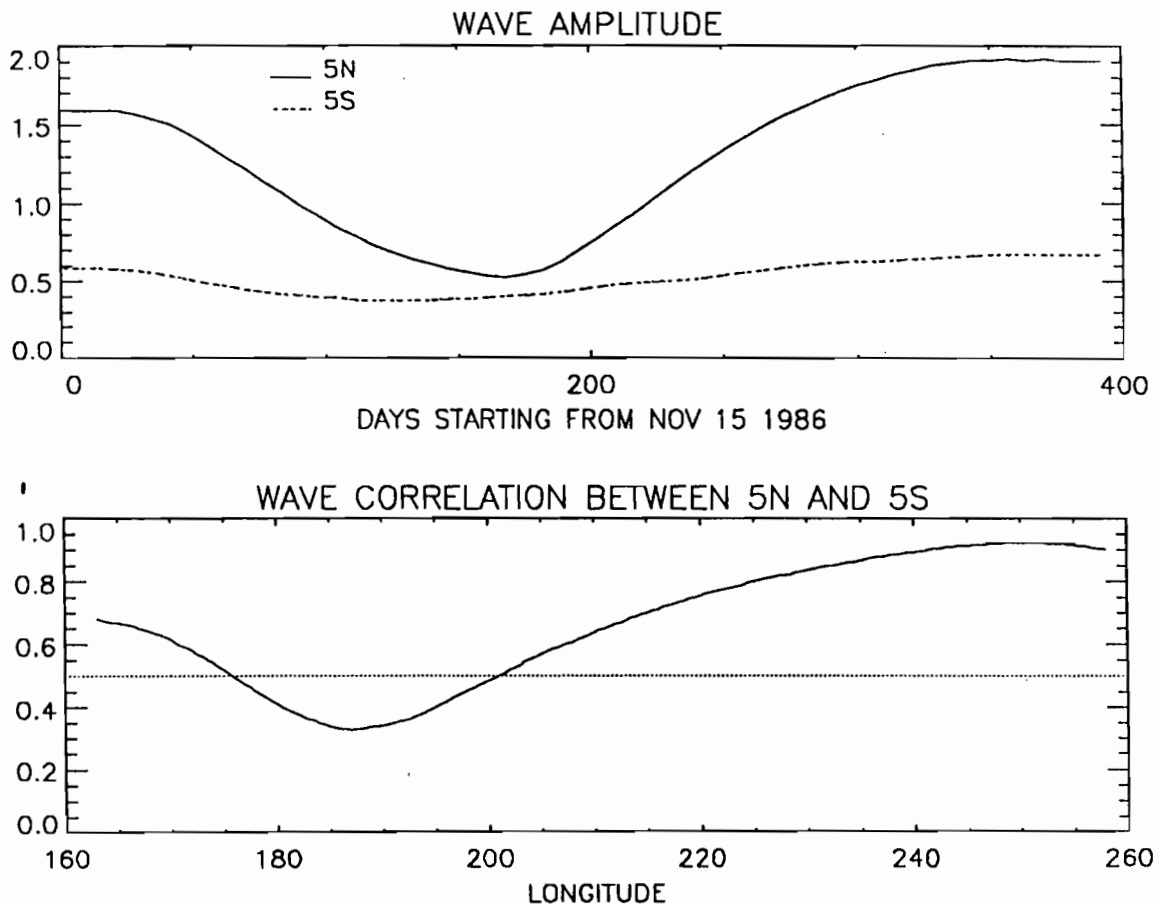


FIG.8. Top: Zonally averaged wave amplitude as a function of time.  
Bottom: correlation in time between wave at 5°N and at 5°S as a function of longitude.



In the East, energy is transported eastward at 35 km/day. Furthermore the strong seasonal modulation is strongly correlated with the increase of shear strength between the South Equatorial Current and the North Equatorial Counter Current as measured by the meridional gradient of sea level derived from Geosat smoothed time series (fig 7 bottom). Indeed the axis along which the shear-strength increases in time by 2 cm per degree of latitude is tilted with time corresponding to a 40 km/day westward migration and its longitude-time location is well correlated with the strengthening of the waves as filtered above.

In the West, the phenomenon look different. The shear strength is increased in winter 1986-1987 when the waves are present but in summer 1987, the shear-strength continues to increase with time as in the East and the waves do not strengthen again before late 1987. Indeed 20 to 30 day oscillations of meridional velocity have been observed in the western Pacific in 1986-1987 with current measurements along the equator and have been correlated with meridional wind fluctuations (McPhaden et al, 1989).

The same filter in frequency and wavenumber has been applied along 5°S. Then no clear eastward nor westward propagation of energy is found. The waves at 5°S show similar seasonal modulation and longitudinal dependency (fig 8 top) but the correlation between 5°N and 5°S is always positive and shows significant symmetry with respect to the equator (fig 8 bottom). The strongest signal in the North with a dominant symmetry can be explained if the waves generated by instability are a superposition of Rossby-Gravity waves and Rossby waves. Similar mechanisms have been invoked in the superposition of Kelvin waves and Rossby waves (Busalacchi et al, 1983).

No evidence for Rossby-gravity wave nor link to the shear-current is demonstrated all across the Pacific. From figure 1 however, the positive anomalies are aligned all across the Pacific along the tilted axis of maximum sheared flow. The filtering zonally applied as previously precludes equatorial convergence of the waves (Schopf et al, 1981). This is why the same frequency-wavenumber band filtering has been applied within a 4° latitudinal band along a tilted axis. Then some energy is gained in the West compared to the previous results but the same time-longitudinal characteristics are found as well.

## VI DISCUSSION

Geosat residuals have been analyzed with different space and time correlation parameters. The different Geosat analyzed series give similar mean RMS differences and similar range of correlation with the tide-gage data, although individual plots show significant differences with the previous ones. Nevertheless negligible difference is found in the spectra in the 10 to 50 day range, as well as in the filtered signal. Thus the previous results are not sensitive to the analysis parameters. This is consistent with the large zonal extent of the tropical waves. However the method used in this study is certainly not optimal to quantify the energy of the instability waves. Both the subsampling of the satellite and the smoothing of the analysis alias the spectra. We must also keep in mind that water vapor content is not properly corrected in Geosat data and that the contribution of the atmospheric signal has not been examined in the present results.

With 13 months of Geosat data, it is possible to describe the time-longitude-latitude extent of the sea level anomaly due to instability waves. Waves with 1000-1500 km, 25 to 45 day, westward 40 km/day phase propagation and eastward 35 km/day energy propagation are clearly present along 5°N East of 160°W all year long except between February and June 1987. Compared to September 1978 as detected from Seasat altimeter (Malarde et al, 1987), these waves are less strong in September 1987. This is consistent with the weaker shear-strength present during the El-Nino 1986-1987 event. Furthermore, altimeter also provides the anomaly of shear-strength of the zonal flow. It is found that for the year 1986-1987, these waves are correlated with an increase of zonal shear East of the dateline and have a more complex latitudinal structure than the Rossby-Gravity wave.

## ACKNOWLEDGEMENTS

The author wants to thank Klaus Wyrtki (University of Hawai, Honolulu) who provided the tide-gage data in the Pacific, Victor Zlotnicki (JPL, Pasadena) who provided the program for orbit error correction, Akiko Hayashi (JPL, Pasadena) who gridded the Geosat GDR along track, and Stuart Pilorz (JPL, Pasadena) who was most helpful in the mathematical analysis. The research described in this paper was carried out by the Jet Propulsion Laboratory, California Institute of Technology, under a contract with the National Aeronautics and Space Administration.

## BIBLIOGRAPHY

BUSALACCHI A.J., TAKEUCHI K. and O'BRIEN J.J., 1983: "Interannual Variability of the Equatorial Pacific - Revisited", *J. Geophys. Res.*, 88, 7551-7562.

CHENEY R.E., DOUGLAS B.C., AGREEN R.W., MILLER L.L., DOYL N.S., 1988: "The NOAA Geosat Geophysical Data Records: summary of the first year of Exact Repeat Mission", NOAA Tech. Memo., NOS-NGS-48, Rockville, MD.

CHENEY R.E., DOUGLAS B.C. and MILLER L., 1989: "Evaluation of Geosat altimeter Data. With application to Tropical Pacific Sea Level Variability", submitted to *J. Geophys. Res.*

CHENEY R.E. and MILLER L., 1987.: "Geosat Altimeter Pacific Ocean Sea Level Anomalies", *Climate Diagnostics Bulletin*, NOAA, Ed: Kousky

COX M.D., 1980: " Generation and Propagation of 30-day waves in a numerical model of the Pacific", *J. Phys. Oceanog.*, 10, 1168-1186.

CRISWELL S.M. and LUKAS R., 1989: "Rossby-gravity Waves in the Central Equatorial Pacific Ocean Durind the NORPAX Hawaii-to-Tahiti Shuttle Experiment", *J. Geophys. Res.*, 2091-2098.

EMERY W., BORN G., BALDWIN D., NORRIS C., 1988: "Satellite based tropospheric water vapor corrections for Geosat altimetry; a comparison between Microwave and Infrared measurements ", *EOS*, 69, 44, 1274.

ENFIELD D., 1987: "The intraseasonal oscillation in eastern Pacific sea levels: How is it forced?", *J. Phys. Oceanog.*, 17,

GASPAR P. and WUNSCH C., 1989: "Estimates from altimeter data of Barotropic Rossby Waves in the Northwestern Atlantic Ocean", submitted to *J. Geophys. Res.*

HALPERN D., KNOX R.A. and LUTHER D.S., 1988: "Observations of 20-day period Meridional current Oscillations in the upper Ocean along the Pacific Equator", *J. Phys. Oceanog.*

HANSON D.V. and PAUL C.A., 1984: "Genesis and effects of long waves in the equatorial Pacific", *J. Geophys. Res.*, 39, 10431-10440.

KENDALL, 1970: "The Pacific Equatorial Countercurrent", Ph D, Nova University.

MALARDE J.P., DE MEY P., PERIGAUD C. and MINSTER J.F., 1987: " The oceanic dynamic topography associated with long equatorial waves", *J. Phys. Oceanog.*, 17, 2273-2279.

McPHADEN M.J., HAYES S.P., MANGUM L.J. and TOOLE J.M., 1989: "Variability in the western Equatorial Pacific Ocean During the 1986-1987 El-Nino/Southern Oscillation Event", submitted to *J. Phys. Oceanog.*

MILLER L., CHENEY R.E. and DOUGLAS B.C., 1988: "Geosat altimeter observations of Kelvin waves and the 1986-1987 El-Nino", *Science*, 239, 52-54.

MILLER L., WATTS D.R. and WIMBUSH M., 1985: "Oscillations of Dynamic topography in the Eastern Equatorial Pacific", *J. Phys. Oceanog.*, 15, 1759-1770.

MITCHUM G.T. and LUKAS R., 1987: "The Latitude-Frequency Structure of Pacific Sea Level Variance", *J. Phys. Oceanog.*, 17, 2362-2365.

SCHOPF P.S., ANDERSON D. and SMITH J., 1981: "Beta Dispersion of low frequency Rossby waves", *Dynamics of Oceans and Atmospheres*, 5, 187-214.

TRIPOLI G.J., and KRISHNAMURTI T.N., 1975: "Low-level flows over the Gate Area during Summer 1972", *Mon. Wea. Rev.*, 197-209.

WEISBERG R.H., 1987: "Observations pertinent to instability waves in the equatorial oceans", *Further Progress in Equatorial Oceanography*, Nova University Press, Edited by Katz and Witte, 335-350.

WEISBERG R.H. and WEINGARTER T.J., 1988: "Instability waves in the equatorial Atlantic Ocean", *J. Phys. Oceanog.*, 1641-1657.

WYRTKI K., 1975: "Fluctuations of the Dynamic Topography in the Pacific Ocean", *J. Phys. Oceanog.*, 5, 450-459.

ZLOTNICKI V., FU L.L., PATZERT W., 1989: "Seasonal variability in global sea level", submitted to *Jour. Geophys. Res.*

**WESTERN PACIFIC INTERNATIONAL MEETING  
AND WORKSHOP ON TOGA COARE**

**Nouméa, New Caledonia**

**May 24-30, 1989**

**PROCEEDINGS**

*edited by*

**Joël Picaut \***

**Roger Lukas \*\***

**Thierry Delcroix \***

\* ORSTOM, Nouméa, New Caledonia

\*\* JIMAR, University of Hawaii, U.S.A.

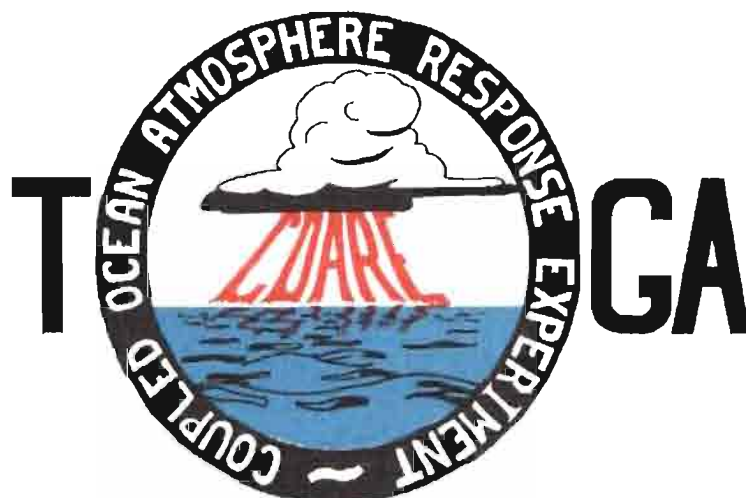


## TABLE OF CONTENTS

<b>ABSTRACT</b> .....	i
<b>RESUME</b> .....	iii
<b>ACKNOWLEDGMENTS</b> .....	vi
<b>INTRODUCTION</b>	
<b>1. Motivation</b> .....	1
<b>2. Structure</b> .....	2
<b>LIST OF PARTICIPANTS</b> .....	5
<b>AGENDA</b> .....	7
<b>WORKSHOP REPORT</b>	
<b>1. Introduction</b> .....	19
<b>2. Working group discussions, recommendations, and plans</b> .....	20
a. Air-Sea Fluxes and Boundary Layer Processes .....	20
b. Regional Scale Atmospheric Circulation and Waves .....	24
c. Regional Scale Oceanic Circulation and Waves .....	30
<b>3. Related programs</b> .....	35
a. NASA Ocean Processes and Satellite Missions .....	35
b. Tropical Rainfall Measuring Mission .....	37
c. Typhoon Motion Program .....	39
d. World Ocean Circulation Experiment .....	39
<b>4. Presentations on related technology</b> .....	40
<b>5. National reports</b> .....	40
<b>6. Meeting of the International Ad Hoc Committee on TOGA COARE</b> .....	40
<b>APPENDIX: WORKSHOP RELATED PAPERS</b>	
<b>Robert A. Weller and David S. Hosom: Improved Meteorological     Measurements from Buoys and Ships for the World Ocean     Circulation Experiment</b> .....	45
<b>Peter H. Hildebrand: Flux Measurement using Aircraft     and Radars</b> .....	57
<b>Walter F. Dabberdt, Hale Cole, K. Gage, W. Ecklund and W.L. Smith:     Determination of Boundary-Layer Fluxes with an Integrated     Sounding System</b> .....	81

## MEETING COLLECTED PAPERS

## WATER MASSES, SEA SURFACE TOPOGRAPHY, AND CIRCULATION

<b>Klaus Wyrtki: Some Thoughts about the West Pacific Warm Pool</b> .....	99
<b>Jean René Donguy, Gary Meyers, and Eric Lindstrom: Comparison of the Results of two West Pacific Oceanographic Expeditions FOC (1971) and WEPOCS (1985-86)</b> .....	111
<b>Dunxin Hu, and Maochang Cui: The Western Boundary Current in the Far Western Pacific Ocean</b> .....	123
<b>Peter Hacker, Eric Firing, Roger Lukas, Philipp L. Richardson, and Curtis A. Collins: Observations of the Low-latitude Western Boundary Circulation in the Pacific during WEPOCS III</b> .....	135
<b>Stephen P. Murray, John Kindle, Dharma Arief, and Harley Hurlburt: Comparison of Observations and Numerical Model Results in the Indonesian Throughflow Region</b> .....	145
<b>Christian Henin: Thermohaline Structure Variability along 165°E in the Western Tropical Pacific Ocean (January 1984 - January 1989)</b> .....	155
<b>David J. Webb, and Brian A. King: Preliminary Results from Charles Darwin Cruise 34A in the Western Equatorial Pacific</b> .....	165
<b>Warren B. White, Nicholas Graham, and Chang-Kou Tai: Reflection of Annual Rossby Waves at The Maritime Western Boundary of the Tropical Pacific</b> .....	173
<b>William S. Kessler: Observations of Long Rossby Waves in the Northern Tropical Pacific</b> .....	185
<b>Eric Firing, and Jiang Songnian: Variable Currents in the Western Pacific Measured During the US/PRC Bilateral Air-Sea Interaction Program and WEPOCS</b> .....	205
<b>John S. Godfrey, and A. Weaver: Why are there Such Strong Steric Height Gradients off Western Australia ?</b> .....	215
<b>John M. Toole, R.C. Millard, Z. Wang, and S. Pu: Observations of the Pacific North Equatorial Current Bifurcation at the Philippine Coast</b> .....	223

## EL NINO/SOUTHERN OSCILLATION 1986-87

<b>Gary Meyers, Rick Bailey, Eric Lindstrom, and Helen Phillips: Air/Sea Interaction in the Western Tropical Pacific Ocean during 1982/83 and 1986/87</b> .....	229
<b>Laury Miller, and Robert Cheney: GEOSAT Observations of Sea Level in the Tropical Pacific and Indian Oceans during the 1986-87 El Nino Event</b> .....	247
<b>Thierry Delcroix, Gérard Eldin, and Joël Picaut: GEOSAT Sea Level Anomalies in the Western Equatorial Pacific during the 1986-87 El Nino, Elucidated as Equatorial Kelvin and Rossby Waves</b> .....	259
<b>Gérard Eldin, and Thierry Delcroix: Vertical Thermal Structure Variability along 165°E during the 1986-87 ENSO Event</b> .....	269
<b>Michael J. McPhaden: On the Relationship between Winds and Upper Ocean Temperature Variability in the Western Equatorial Pacific</b> .....	283

<b>John S. Godfrey, K. Ridgway, Gary Meyers, and Rick Bailey:</b> Sea Level and Thermal Response to the 1986-87 ENSO Event in the Far Western Pacific .....	291
<b>Joël Picaut, Bruno Camusat, Thierry Delcroix, Michael J. McPhaden, and Antonio J. Busalacchi:</b> Surface Equatorial Flow Anomalies in the Pacific Ocean during the 1986-87 ENSO using GEOSAT Altimeter Data .....	301

#### THEORETICAL AND MODELING STUDIES OF ENSO AND RELATED PROCESSES

<b>Julian P. McCreary, Jr.:</b> An Overview of Coupled Ocean-Atmosphere Models of El Nino and the Southern Oscillation .....	313
<b>Kensuke Takeuchi:</b> On Warm Rossby Waves and their Relations to ENSO Events .....	329
<b>Yves du Penhoat, and Mark A. Cane:</b> Effect of Low Latitude Western Boundary Gaps on the Reflection of Equatorial Motions .....	335
<b>Harley Hurlburt, John Kindle, E. Joseph Metzger, and Alan Wallcraft:</b> Results from a Global Ocean Model in the Western Tropical Pacific .....	343
<b>John C. Kindle, Harley E. Hurlburt, and E. Joseph Metzger:</b> On the Seasonal and Interannual Variability of the Pacific to Indian Ocean Throughflow .....	355
<b>Antonio J. Busalacchi, Michael J. McPhaden, Joël Picaut, and Scott Springer:</b> Uncertainties in Tropical Pacific Ocean Simulations: The Seasonal and Interannual Sea Level Response to Three Analyses of the Surface Wind Field .....	367
<b>Stephen E. Zebiak:</b> Intraseasonal Variability - A Critical Component of ENSO ? .....	379
<b>Akimasa Sumi:</b> Behavior of Convective Activity over the "Jovian-type" Aqua-Planet Experiments .....	389
<b>Ka-Ming Lau:</b> Dynamics of Multi-Scale Interactions Relevant to ENSO .....	397
<b>Pecheng C. Chu and Roland W. Garwood, Jr.:</b> Hydrological Effects on the Air-Ocean Coupled System .....	407
<b>Sam F. Iacobellis, and Richard C.J. Somerville:</b> A one Dimensional Coupled Air-Sea Model for Diagnostic Studies during TOGA-COARE .....	419
<b>Allan J. Clarke:</b> On the Reflection and Transmission of Low Frequency Energy at the Irregular Western Pacific Ocean Boundary - a Preliminary Report .....	423
<b>Roland W. Garwood, Jr., Pecheng C. Chu, Peter Muller, and Niklas Schneider:</b> Equatorial Entrainment Zone : the Diurnal Cycle .....	435
<b>Peter R. Gent:</b> A New Ocean GCM for Tropical Ocean and ENSO Studies .....	445
<b>Wasito Hadi, and Nuraini:</b> The Steady State Response of Indonesian Sea to a Steady Wind Field .....	451
<b>Pedro Ripa:</b> Instability Conditions and Energetics in the Equatorial Pacific .....	457
<b>Lewis M. Rothstein:</b> Mixed Layer Modelling in the Western Equatorial Pacific Ocean .....	465
<b>Neville R. Smith:</b> An Oceanic Subsurface Thermal Analysis Scheme with Objective Quality Control .....	475
<b>Duane E. Stevens, Qi Hu, Graeme Stephens, and David Randall:</b> The hydrological Cycle of the Intraseasonal Oscillation .....	485
<b>Peter J. Webster, Hai-Ru Chang, and Chidong Zhang:</b> Transmission Characteristics of the Dynamic Response to Episodic Forcing in the Warm Pool Regions of the Tropical Oceans .....	493

## MOMENTUM, HEAT, AND MOISTURE FLUXES BETWEEN ATMOSPHERE AND OCEAN

<b>W. Timothy Liu: An Overview of Bulk Parametrization and Remote Sensing of Latent Heat Flux in the Tropical Ocean</b> .....	513
<b>E. Frank Bradley, Peter A. Coppin, and John S. Godfrey: Measurements of Heat and Moisture Fluxes from the Western Tropical Pacific Ocean</b> .....	523
<b>Richard W. Reynolds, and Ants Leetmaa: Evaluation of NMC's Operational Surface Fluxes in the Tropical Pacific</b> .....	535
<b>Stanley P. Hayes, Michael J. McPhaden, John M. Wallace, and Joël Picaut: The Influence of Sea-Surface Temperature on Surface Wind in the Equatorial Pacific Ocean</b> .....	543
<b>T.D. Keenan, and Richard E. Carbone: A Preliminary Morphology of Precipitation Systems In Tropical Northern Australia</b> .....	549
<b>Phillip A. Arkin: Estimation of Large-Scale Oceanic Rainfall for TOGA</b> .....	561
<b>Catherine Gautier, and Robert Frouin: Surface Radiation Processes in the Tropical Pacific</b> .....	571
<b>Thierry Delcroix, and Christian Henin: Mechanisms of Subsurface Thermal Structure and Sea Surface Thermo-Haline Variabilities in the South Western Tropical Pacific during 1979-85 - A Preliminary Report</b> .....	581
<b>Greg. J. Holland, T.D. Keenan, and M.J. Manton: Observations from the Maritime Continent : Darwin, Australia</b> .....	591
<b>Roger Lukas: Observations of Air-Sea Interactions in the Western Pacific Warm Pool during WEPOCS</b> .....	599
<b>M. Nunez, and K. Michael: Satellite Derivation of Ocean-Atmosphere Heat Fluxes in a Tropical Environment</b> .....	611

## EMPIRICAL STUDIES OF ENSO AND SHORT-TERM CLIMATE VARIABILITY

<b>Klaus M. Weickmann: Convection and Circulation Anomalies over the Oceanic Warm Pool during 1981-1982</b> .....	623
<b>Claire Perigaud: Instability Waves in the Tropical Pacific Observed with GEOSAT</b> .....	637
<b>Ryuichi Kawamura: Intraseasonal and Interannual Modes of Atmosphere-Ocean System Over the Tropical Western Pacific</b> .....	649
<b>David Gutzler, and Tamara M. Wood: Observed Structure of Convective Anomalies</b> .....	659
<b>Siri Jodha Khalsa: Remote Sensing of Atmospheric Thermodynamics in the Tropics</b> .....	665
<b>Bingrong Xu: Some Features of the Western Tropical Pacific: Surface Wind Field and its Influence on the Upper Ocean Thermal Structure</b> .....	677
<b>Bret A. Mullan: Influence of Southern Oscillation on New Zealand Weather</b> .....	687
<b>Kenneth S. Gage, Ben Basley, Warner Ecklund, D.A. Carter, and John R. McAfee: Wind Profiler Related Research in the Tropical Pacific</b> .....	699
<b>John Joseph Bates: Signature of a West Wind Convective Event in SSM/I Data</b> .....	711
<b>David S. Gutzler: Seasonal and Interannual Variability of the Madden-Julian Oscillation</b> .....	723
<b>Marie-Hélène Radenac: Fine Structure Variability in the Equatorial Western Pacific Ocean</b> .....	735
<b>George C. Reid, Kenneth S. Gage, and John R. McAfee: The Climatology of the Western Tropical Pacific: Analysis of the Radiosonde Data Base</b> .....	741



<b>Chung-Hsiung Sui, and Ka-Ming Lau: Multi-Scale Processes in the Equatorial Western Pacific</b> .....	747
<b>Stephen E. Zebiak: Diagnostic Studies of Pacific Surface Winds</b> .....	757

#### MISCELLANEOUS

<b>Rick J. Bailey, Helene E. Phillips, and Gary Meyers: Relevance to TOGA of Systematic XBT Errors</b> .....	775
<b>Jean Blanchot, Robert Le Borgne, Aubert Le Bouteiller, and Martine Rodier: ENSO Events and Consequences on Nutrient, Planktonic Biomass, and Production in the Western Tropical Pacific Ocean</b> .....	785
<b>Yves Dandonneau: Abnormal Bloom of Phytoplankton around 10°N in the Western Pacific during the 1982-83 ENSO</b> .....	791
<b>Cécile Dupouy: Sea Surface Chlorophyll Concentration in the South Western Tropical Pacific, as seen from NIMBUS Coastal Zone Color Scanner from 1979 to 1984 (New Caledonia and Vanuatu)</b> .....	803
<b>Michael Szabados, and Darren Wright: Field Evaluation of Real-Time XBT Systems</b> .....	811
<b>Pierre Rual: For a Better XBT Bathy-Message: Onboard Quality Control, plus a New Data Reduction Method</b> .....	823